0 0 0 0 1 0 0 0 0 2

Submitted to the JOURNAL OF THE OPTICAL
SOCIETY OF AMERICA

LBL-8021 c.1
Preprint
CC-34a

FIRST IONIZATION POTENTIALS OF LANTHANIDES BY LASER SPECTROSCOPY

E. F. Worden, R. W. Solarz, J. A. Paisner and J. G. Conway

July, 1978

Prepared for the U. S. Department of Energy
under Contract W-7405-ENG-48

For Reference

Not to be taken from this room

LAWRENCE BERKELEY LABORATORY
UNIVERSITY OF CALIFORNIA
BERKELEY

RECEIVED
LAWRENCE
BERKELEY LABORATORY

JAN 29 1979

LIBRARY AND
DOCUMENTS SECTION

LBL-8021 c.1

DISCLAIMER

This document was prepared as an account of work sponsored by the United States Government. While this document is believed to contain correct information, neither the United States Government nor any agency thereof, nor the Regents of the University of California, nor any of their employees, makes any warranty, express or implied, or assumes any legal responsibility for the accuracy, completeness, or usefulness of any information, apparatus, product, or process disclosed, or represents that its use would not infringe privately owned rights. Reference herein to any specific commercial product, process, or service by its trade name, trademark, manufacturer, or otherwise, does not necessarily constitute or imply its endorsement, recommendation, or favoring by the United States Government or any agency thereof, or the Regents of the University of California. The views and opinions of authors expressed herein do not necessarily state or reflect those of the United States Government or any agency thereof or the Regents of the University of California.

First ionization potentials of lanthanides by laser spectroscopy*

E. F. Worden, R. W. Solarz, J. A. Paisner
Lawrence Livermore Laboratory, Livermore, California 94550
J. G. Conway
Lawrence Berkeley Laboratory, Berkeley, California 94720
(Received 9 September 1977)

Photoionization and Rydberg spectra of ten lanthanides have been studied using stepwise laser excitation and ionization methods. These spectra were obtained from several different laser populated excited states in each case. Accurate ionization limits were derived from observed photoionization thresholds. Except for praseodymium, the observation of one or more long Rydberg progressions allowed more accurate limits to be determined. The Rydberg convergence values in eV are: Ce, 5.5387(4); Nd, 5.5250(6); Sm, 5.6437(6); Eu, 5.6704(3); Gd, 6.1502(6); Tb, 5.8639(6); Dy, 5.9390(6); Ho, 6.0216(6), and Er 6.1077(10). For praseodymium a threshold value of $5.464(^{+12}_{-2})$ eV was obtained. When plotted against N, the lanthanide ionization limits normalized to correspond to ionization from the lowest level of $f^N s^2$ to the lowest level of $f^N s$ form two straight lines connected at the half-filled shell.

INTRODUCTION

Ionization potentials are important physical properties of atoms. They aid in identifying systematic trends in binding energies from element to element and are useful in the interpretation of atomic spectra. Accurate values are required to determine the extent of ionization of high temperature gas mixtures containing the atoms.

The most accurate atomic ionization limits are determined from the measurement of long Rydberg series. Another technique used for obtaining ionization limits, although less accurate, is the determination of the ionization threshold. In the lanthanides, with the exception of the few with simple spectra, obtaining these measurements by conventional methods is difficult, if not impossible. Thus, accurate ionization limits are not available for the majority of the lanthanides.[1]

The difficulty in observing Rydberg series in most lanthanides arises from the extreme complexity of their electronic structure. The spectra of these elements are very dense and are characterized by weak absorptions, especially into Rydberg levels with large principal quantum numbers. The presence of a number of thermally populated low-lying levels in most of the atoms of these elements together with the great density of potentially perturbing valence levels at high energy so complicates most of the single photon absorption spectra that Rydberg series cannot be identified. Indeed, the only lanthanides where Rydberg series have been observed by conventional spectroscopy[2–5] have relatively simple spectra and very few low-lying energy levels.[6] The elements lanthanum,[2] europium,[3] thulium,[4] ytterbium,[5] and lutetium[5] all have only one or two well-isolated low levels that are thermally populated at the temperatures needed to produce an atomic vapor and have only a few well-separated ion levels to serve as Rydberg convergence limits. For the remaining elements with complex spectra, more sensitive and flexible methods are required for the observation of well-developed Rydberg series.

The same arguments apply to the study of ionization thresholds. While some success has been possible for the elements with simpler electronic structure (ytterbium, europium, and thulium),[7,8] for the remainder of the lanthanides it is nearly an impossible task to unravel the spectra originating from the many populated metastable levels to accurately determine the ionization limit with confidence.[9]

Recently, stepwise laser photoexcitation and ionization has been used in our laboratory to identify Rydberg series in atomic uranium.[10] The methods offer a number of advantages over conventional techniques. They allow the high-lying levels connected by optical transitions to the ground level or to any of the low-lying thermally populated metastable levels to be selectively excited. The excitation may take place in a single step or in two steps to reach the desired level. Spectra obtained from these laser prepared excited levels are not subject to the ambiquities associated with conventional absorption and ionization spectra. One clearly avoids the difficulty of sorting out which of the thermally populated low-lying levels is associated with a specific feature of the spectrum. The methods are sensitive because of the spectral intensity of lasers and the use of ion detection. When required, time delaying the ionization step can be used as a discriminant to preferentially detect the long-lived Rydberg levels. These methods are similar to those used by Dunning and Stebbings.[11]

We have applied these multistep photionization methods to obtain Rydberg series and photoionization thresholds in the lanthanides. This has permitted us to obtain accurate ionization limits for ten lanthanides. When these results are combined with the available literature values,[1–5] accurate experimental ionization potentials become available for all the lanthanides except promethium. These ionization limits, when normalized to correspond to the energy between the lowest level of the $f^N s^2$ configuration of the neutral and the lowest level of the $f^N s$ configuration of the ion, and when plotted against N, display a connected two-straight-line behavior with a slope change at the half-filled shell. Theory predicts such a behavior for lowest level to lowest level ionization potential for $l^N s^2 \rightarrow l^N s$ configurations.

EXPERIMENTAL

The experimental apparatus used is shown schematically in Fig. 1 and is similar to ones described previously.[10,12] It is a crossed beam spectrometer in which the atoms in the

 0030-3941/78/6801-0052$00.50 © 1978 Optical Society of America

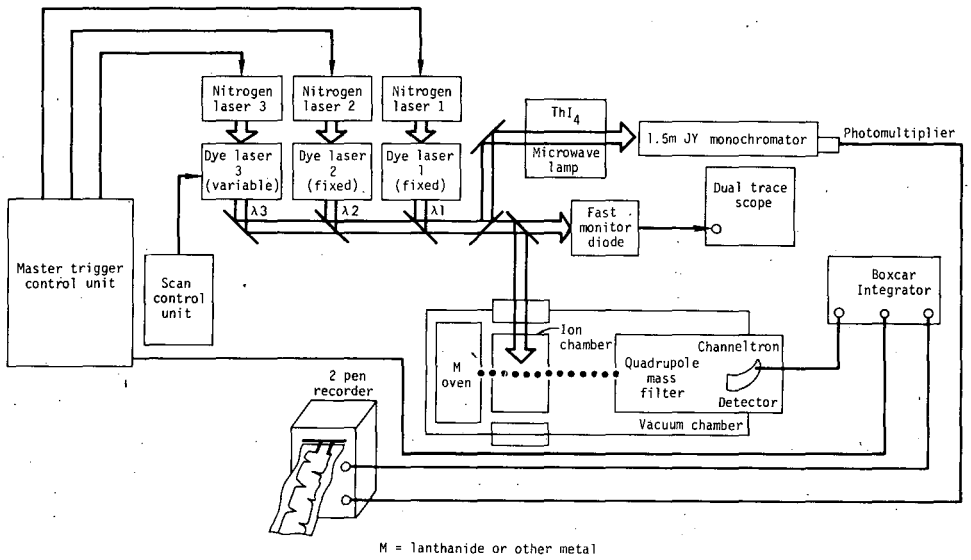

FIG. 1. Laser spectroscopy apparatus.

atomic beam are irradiated and eventually ionized by the output of either two or three commercial nitrogen (Molectron UV-400) laser-pumped tunable dye lasers (Molectron DL-200). The oven consists of a resistively heated tungsten tube containing a tungsten crucible holding the metal to be vaporized. The oven is usually operated at a temperature sufficient to give an atomic vapor pressure of roughly 10^{-3} Torr. The vapor effuses through a slit into an interaction chamber where, at an atom density of approximately 10^9 to 10^{11} atoms/cm^3, it is irradiated by the dye laser pulses. The chamber is electrically biased to suppress thermal and surface ions and to efficiently collect and direct photoion products into the detection system. The detector is a channeltron particle multiplier at −2900 V contained in an Extranuclear Model No. 324-9 quadrupole mass analyzer. The quadrupole is tuned to the mass of the atom under study and thus serves to discriminate against detection of oxide or other impurities. The vacuum chamber background pressure is typically 10^{-7} Torr.

The interaction chamber-quadrupole setup can be replaced by a field ionization chamber and channeltron ion detector. The field ionization chamber consists of a gold-plated copper capacitor anode plate separated by 1 cm from a 50 mesh stainless steel grid maintained at ground potential. A channeltron is located behind the grid to detect the ions produced by the pulsed electric field. The field acts to both produce and deflect the ions into the negatively biased channeltron. The pulsed electric field could be varied from 0 to 5 kV and had a rise time of less than 50 ns with a pulse width variable between 0.1 and 100 μs. The pulse could be delayed with respect to the final laser by 0–10 μs. Since there was no mass filtering when the field-ionization apparatus was employed, any oxide contamination is a potential source of background photoion signal. In these cases the metallic sample was baked in vacuum for several hours to drive off the higher vapor pressure oxides.

The nitrogen pump lasers are triggered by a common master control unit so that each laser fires at predetermined and well-controlled times with respect to the others. The desired time delay and sequencing between the outputs of the N_2 lasers was obtained by inserting an appropriate length of cable in the trigger circuit. The dye laser pulses were monitored by a fast vacuum photodiode (ITT No. FW-114A) and displayed on a Tektronix 7904 oscilloscope. Typically, the jitter between the time-delayed dye laser pulses was less than 5 ns. The dye lasers provided 5–10 ns pulses having 0.5–2.0 cm^{-1} spectral linewidths. The master control unit also gated the boxcar (Princeton Applied Research Model No. 162) that integrated the signal received from the particle multiplier.

The first and/or second dye lasers were tuned to the specific wavelength(s) to populate the desired level(s). The final laser in the excitation sequence (either the second or third laser) was then continuously scanned to obtain the Rydberg or autoionization spectrum. In all cases, the spectrum was obtained by monitoring the ionization yield as a function of the scanning laser wavelength. This spectrum and wavelength calibrations were recorded simultaneously on a two pen recorder. Wavelength calibration was obtained by directing a portion of the scan laser radiation to a 1.5 m Jobin-Yvon monochromator that was preset at known U or Th emission lines from an electrodeless lamp.

The excitation schemes employed to obtain photoionization

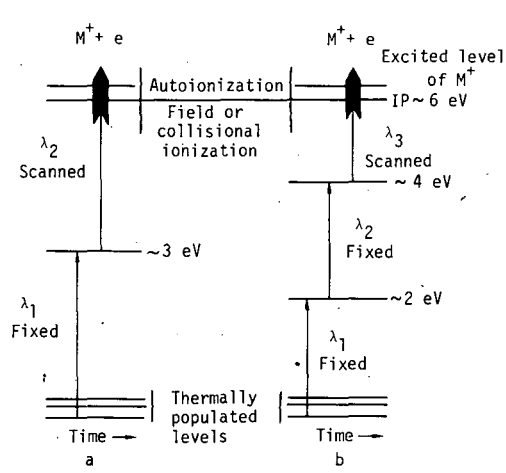

FIG. 2. Excitation schemes used to obtain Rydberg and autoionization spectra.

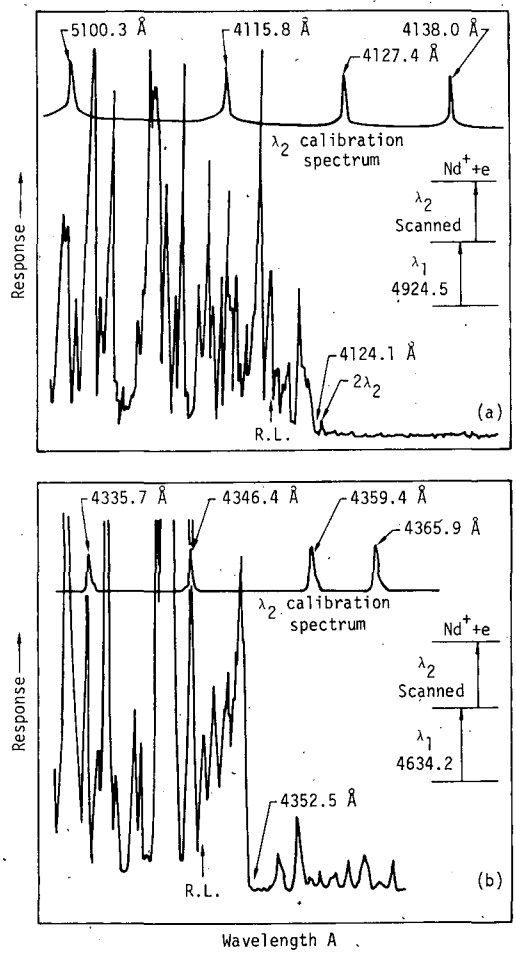

FIG. 3. Photoionization threshold spectra for neodymium. The excitation scheme used in each case is shown on the figure. The scanned laser wavelength calibration is shown at the top of each spectrum. In (a) the 20 300.8 cm^{-1} level, is populated and in (b) the 21 572.6 cm^{-1} level is populated. The threshold wavelengths indicated yield the same ionization limit value of 5.523 eV. The arrows labeled R.L. indicate the position of the Rydberg convergence limit.

and Rydberg spectra are indicated in Fig. 2. A time delay of 10–20 ns was introduced between laser outputs to provide an unambiguous excitation sequence. The primary excitation (λ_1) was always a known transition from the ground or low-lying thermally populated level. (In our notation λ_i is the wavelength of the ith laser in the excitation sequence.) In the three-step experiments λ_2 was usually a known transition, but occasionally it was necessary to use a transition obtained by laser spectroscopy techniques where λ_1 was fixed, λ_2 was scanned, and λ_3 was fixed at a wavelength such that the energy of $\lambda_1 + \lambda_2 + \lambda_3$ exceeded the ionization potential of the element. Ion current was obtained when λ_2 coincided with an allowed transition from the level populated by λ_1. A more detailed description of this method has been given previously.[12] Such searches were performed whenever there were not a sufficient number of known levels in the 3–4 eV range to obtain Rydberg or photoionization threshold spectra.

Background peaks could occur in all spectra obtained. For two laser excitations and depending on the wavelengths of λ_1 and λ_2, $2\lambda_2$ peaks from the ground or thermally populated levels or $3\lambda_2$ peaks could be present. When using 3 lasers, $\lambda_1 + 2\lambda_3$ or $3\lambda_3$ peaks could occur. Background scans were performed by blocking λ_1 and/or λ_2 and repeating the λ_2 or λ_3 scan to determine those peaks that were not due to the desired $\lambda_1 + \lambda_2$ or $\lambda_1 + \lambda_2 + \lambda_3$ sequence in each case.

The usual procedure was to first identify the photoionization threshold from one or more excited levels of the atom under study using the two-step method (Fig. 2a). This involved scanning a considerable range estimated from the available literature values[1,13,14] that had quoted uncertainties as large as ± 800 cm^{-1}. The most recent compilation of values based on spectroscopic data[1] had quoted uncertainties of about ± 200 cm^{-1} and in most cases the thresholds were found within the ranges estimated from these values. Thresholds were also observed using the three-step method (Fig. 2b) to confirm and improve some of the two-step results. Once the photoionization threshold limit was obtained to an accuracy of about 30 cm^{-1} for an element, wavelength ranges to search for bound Rydberg series with field or collisional ionization or to search for autoionizing series converging to excited states of the ion were estimated for various parent levels that could be conveniently populated by one- or two-step excitation. Scans were made from various parent levels until series were obtained. The success rate for such scans varied from element to element, but overall approximately one-third of the scans were successful.

As indicated in Fig. 2, several methods of ionization were employed to observe series. In most cases (Nd, Sm, Eu, Dy, Ho, and Er) autoionizing Rydberg series converging to an excited state of the ion were obtained. For lanthanides where the autoionizing Rydberg series are obscured by the high density of autoionizing valence states, field ionization was used. This was the case for cerium, gadolinium, and terbium. The field was applied 2–5 μs after the populating laser λ_2 or λ_3. This time resolution allowed radiative decay of some of the shorter-lived valence levels and facilitiated preferential detection of longer-lived Rydberg levels. Collisional ionization was used to observe a series in holmium. In this case, the oven temperature was increased until the atom density was such that the bound Rydberg levels were ionized and a long series was obtained.

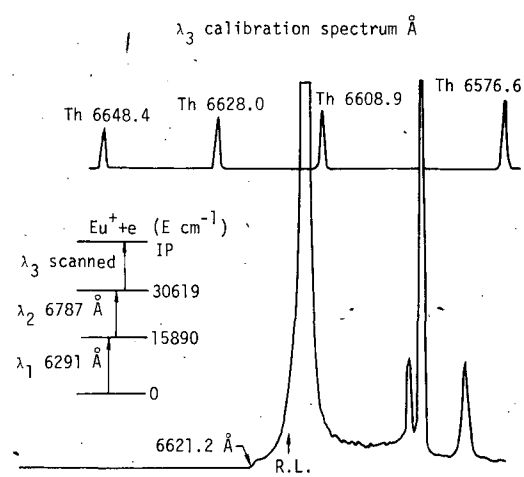

FIG. 4. Photoionization threshold spectrum for europium. The excitation scheme is shown on figure. The scanned laser wavelength calibration spectrum is shown at the top of the figure. The arrow labeled R.L. indicates the position of the Rydberg convergence limit.

TABLE I. Two-step photoionization threshold results. The numbers in parentheses following values in the table are the uncertainty in the last digit of that value.

Element	Excitation wavelength, λ_1[a] (Å)	Excited level used[a] (cm^{-1})	λ_2-Wavelength at threshold (Å)	Ionization threshold[b,c] (cm^{-1})	(eV)
Ce	4583.10	21 813.23	4370.7	44 686(40)	5.540(5)
	4610.46	21 683.74	4351.7	44 657(40)	5.537(5)
	4632.32	21 581.41	4338.2	46 626(40)	5.533(5)
Pr	3945.41	26 715.34	5762	44 065($^{+100}_{-20}$)	5.463($^{+12}_{-2}$)
	4939.74	23 085.08	4764	44 070($^{+100}_{-20}$)	5.464($^{+12}_{-2}$)
Nd	4634.24	21 572.61	4352.2	44 543(15)	5.523(2)
	4924.53	20 300.84	4124.1	44 542(15)	5.522(2)
	4954.78	20 176.90	4103.4	44 543(15)	5.523(2)
	5056.89	19 769.49	4352.2	44 543(15)	5.523(2)
Sm	4226.18	24 467.27	4756.7	45 484(15)	5.639(2)
	4596.74	22 041.02	4263.2	45 491(15)	5.640(2)
Eu	4594.03	21 761.26	4181.0	45 672(30)	5.663(4)
	4661.88	21 444.58	4118.2	45 720(30)	5.669(4)
Dy	4565.09	21 899.22	3847.5	47 882(25)	5.937(3)
	4589.35	21 783.42	3831.1	47 879(25)	5.936(3)
	4612.26	21 675.28	3820.5	47 843(25)	5.631(3)
Ho	4040.81	24 740.52	4206.0	48 509(25)	6.014(3)
	4053.93	24 660.46	4185.5	48 546(25)	6.019(3)
Er	4087.63	24 457.15	4034.2	49 238(15)	6.105(2)

[a]Excitation wavelengths (λ_1) and excited level values are from Ref. 15 and references therein.
[b]Uncertainties are generally larger than the precision of individual threshold determinations. They are set so that application of the uncertainty results in overlap of the values.
[c]8065.479 cm^{-1}/eV was used to convert the values from cm^{-1} to eV.

RESULTS

A. Photoionization threshold spectra

Neodymium photoionization spectra from two different parent levels are shown in Fig. 3. The excitation sequences are shown on the figure. The thresholds are marked by the onset of very strong autoionizing transitions. In addition, weak background due to continuum ionization is present. Scan (a) shows very few ionization peaks of the type $\lambda_1 + 2\lambda_2$ before the onset of $\lambda_1 + \lambda_2$ ionization so that the threshold is very easily recognized. In scan (b) a number of $\lambda + 2\lambda_2$ peaks precede the threshold but the strength of the autoionizing peaks and continuous absorption make identification of the threshold easy. For Ce, Pr, and Ho, the presence of background peaks made identification somewhat more difficult. The spectrum for europium shown in Fig. 4 exhibits very few autoionization peaks and the threshold is identified by the weak continuous photoionization background. This is in contrast to the neodymium spectra (Fig. 3) where the density of well-defined autoionization peaks approaches the instrumental resolution. The density of autoionizing transitions of each element was found to follow roughly the complexity of the level structure as revealed by the analysis of the emission spectra.[6] Except for europium, the lanthanides we investigated exhibit autoionization spectra near the threshold similar to neodymium.

The photoionization threshold results are given in Tables I and II for the two- and three-step measurements, respec-

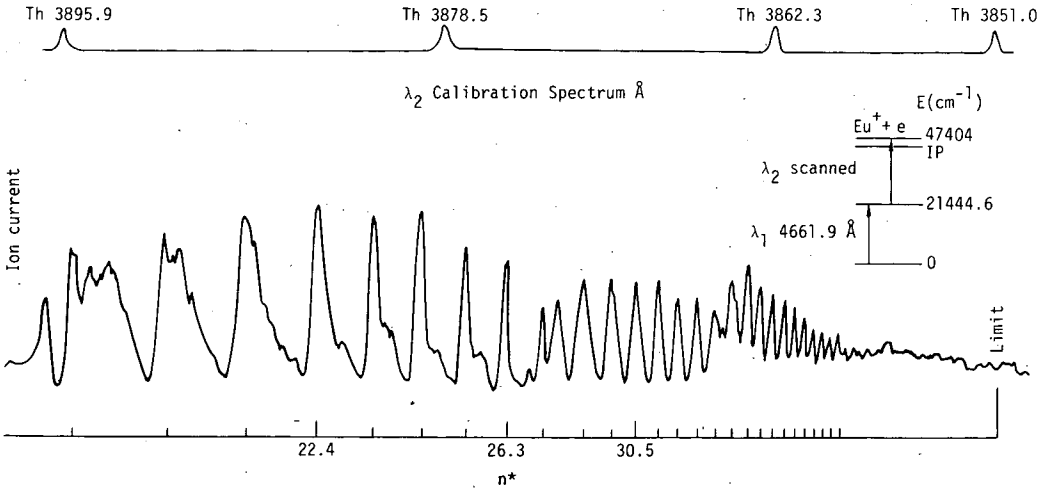

FIG. 5. Europium autoionizing Rydberg series from the $^8P_{5/2}$ level at 21 444 cm^{-1} converging to the $^7S_3^o$ limit 1669.2 cm^{-1} above the $^9S_4^o$ ground state of the ion.

TABLE II. Three-step photoionization threshold results. The numbers in parentheses in the table are the uncertainty in the last place of the value it follows.

Element	Excitation Wavelengths[a] λ_1 (Å)	λ_1 (Å)	Excited level used[a] (cm^{-1})	λ_3 Wavelength at threshold (Å)	Ionization threshold[b,c] (cm^{-1})	(eV)
Ce	6310.10	6996.8	30 131(2)	6883.0	44 656(40)	5.539(5)
Eu	6291.34	6787.48	30 619.49	6621.2	45 718(30)	5.668(4)
Dy	6259.09	6769.79	30 739.79	5831.1	47 884(25)	5.937(3)
Ho	6305.36	6576.8	31 056(2)	5720.0	48 534(25)	6.017(3)
	6305.36	6901.1	30 342(2)	5495.0	48 535(25)	6.018(3)
	6305.36	6947.1	30 246(2)	5462.1	48 549(25)	6.019(3)
Er	6221.02	6388.19	31 719.65	5706.8	49 238(15)	6.105(2)
	6221.02	6451.56	31 565.94	5655.6	49 243(15)	6.105(2)
	6221.02	6649.06	31 105.66	5516.1	49 230(15)	6.104(2)

[a]Excitation wavelengths (λ_1 and λ_2) and excited level values are from Ref. 15 and references therein except for Ce and Ho which were determined by laser techniques, Ref. 12.
[b]Uncertainties are generally larger than the precision of individual threshold determinations. They are set so that application of the uncertainty results in overlap of the values.
[c]8065.479 cm^{-1}/eV was used to convert the cm^{-1} values to eV.

tively. The excitation wavelengths in column two of Table I correspond to transitions from the ground or a thermally populated metastable level to the excited levels in column three. In Table II the two wavelengths necessary to access the excited level used are given in the columns headed "Excitation wavelengths." The last three columns in the tables give the observed wavelength in angstroms of the scanned laser at the onset of photoionization and the corresponding value of the ionization threshold from the ground state of the element in wave numbers and in eV.

For each element, more than one excitation sequence was used to observe the threshold. The single uncertainties quoted in Tables I and II for each of the measurements of the ionization thresholds for a given element were set so that there was overlap of the values within that uncertainty. They are not indicative of the precision of determination of individual threshold values which was about 5–10 cm^{-1} depending on the element and the transition sequence. The variation in threshold values obtained from different parent levels of the same element results from differences in the photoionization structure near the threshold. Even with the larger uncertainties adopted, the threshold limits were 10 times more accurate than the values available in the literature.[1] Their determinations reduced the search ranges for Rydberg levels to reasonable values. Because the Rydberg convergence limits are much more accurate, the uncertainties in the threshold values are not consequential, with the exception of praseodymium where Rydberg series were not obtained. The uncertainty established for the threshold limit of praesodymium is −20 to +100 cm^{-1} as explained in the Discussion section.

B. Rydberg series spectra

Typical Rydberg spectra obtained for Eu, Dy, Ho, and Ce are shown in Figs. 5–8. The excitation sequences used in each case are included on the figures. The europium and dysprosium spectra are both autoionizing Rydberg series converging to the first excited state of the ion. The europium series shows about 27 members before the spacing between

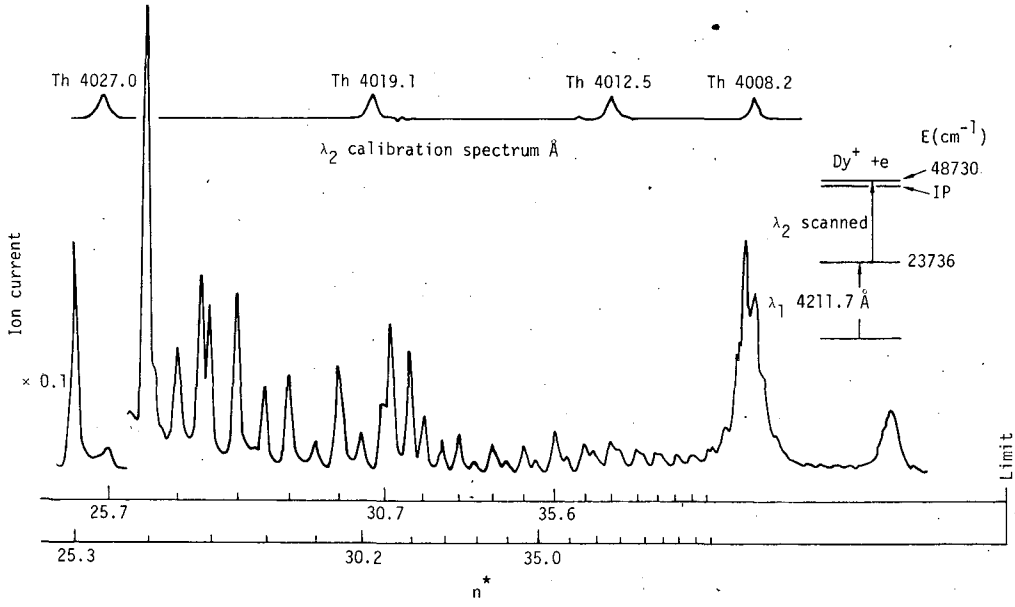

FIG. 6. Dysprosium autoionizing Rydberg series converging to the $^4i_{15/2}$ limit 828.3 cm^{-1} above the $^6I_{17/2}$ ground state of the ion. This is a double series converging to the same limit.

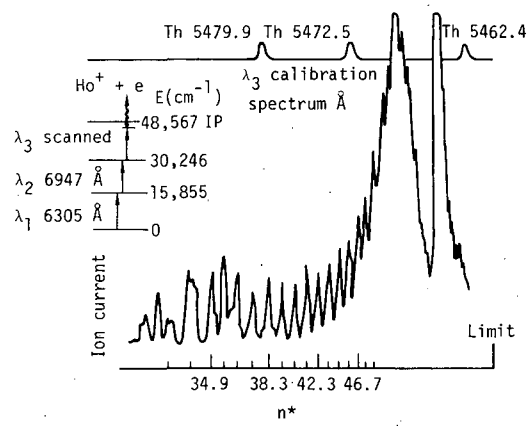

FIG. 7. Collisionally ionized Rydberg series of holmium converging to the $^5I_8^o$ ground state of the ion. The excitation sequence is shown with collision ionization indicated by the wavy arrow.

levels becomes equivalent to the dye laser bandwidth. The series was observed from the $4f^76s6p\,^8P_{5/2}$ level at 21 444 cm^{-1} and could be a $4f^76sns$ or $4f^76snd$ series. It is relatively free from autoionizing valence levels and has the same general appearance as the more extensive autoionizing series observed by Smith and Tomkins[3] using conventional absorption spectroscopy. The lower members of the series are broadened by the increased splitting at lower n of the complex structure of each Rydberg level. If the series is a $4f^76s(^7S)nd$ series, then in LS coupling each Rydberg term would consist of the 6 levels $^6D_{3/2,5/2,7/2}$, $^8D_{3/2,5/2,7/2}$. There is no reason to believe LS or any particular coupling scheme should be appropriate for these excited levels in the lanthanides. Regardless of the coupling scheme, all the series members observed here for the lanthanides are complex terms that consist of many channels that are unresolved at high n values with the laser widths used ($\sim$1 cm^{-1}).

The dysprosium Rydberg spectrum is a double series converging to the $4f^{10}6s\ ^4I_{15/2}$ limit 828.31 cm^{-1} above the ground level of the ion. The dysprosium spectrum is also relatively free from perturbing and obscuring autoionizing levels. Well-developed autoionizing Rydberg series were also obtained for Nd, Sm, and Er. However, some of these spectra showed more obscuring and perturbing autoionizing levels. Nevertheless, all the spectra obtained had clearly discernible autoionizing Rydberg series with 10–25 observed members.

The collisionally ionized Rydberg series obtained for holmium is shown in Fig. 7. This is a bound series converging to the $4f^{11}6s\ ^5I_8^o$ ground state of the ion. The two broad intense features in the spectrum before the limit is reached deserve comment. Similar features were observed in the europium absorption spectrum by Smith and Tomkins[3] who attributed the features to buildup of intensity due to closely spaced Rydberg terms. The same explanation cannot be offered for our observations because the density of observed Rydberg levels at the long wavelength feature is not sufficient to account for the very rapid increase in intensity. Certainly a possible explanation for the double-peaked envelope is a rapid variation of the collisional ionization cross section with n. However, the most plausible explanation is that the intensity variations are due to the presence of other levels interacting with the Rydberg levels to produce intensity perturbations. Further investigation of these features appears necessary for a full understanding of the observation.

The cerium Rydberg series shown in Fig. 8 was obtained by field ionization. The field strength was 100 V/cm and the pulse was delayed by 4 μs from the populating laser λ_2. The series consists of twenty clearly resolved members with n^* values from 38.6 to 58.6.

C. Rydberg convergence limits

The variation in quantum defect $(n - n^*)$ vs n with change in assumed limit value for cerium is shown in Fig. 9. The value of n is not necessarily the principal quantum number but is an integer chosen close to n^* in order to evaluate the variation in quantum defect. The effective quantum number n^* is obtained from $n^* = \{R/[\text{assumed limit} - \text{level value}]\}^{1/2}$,

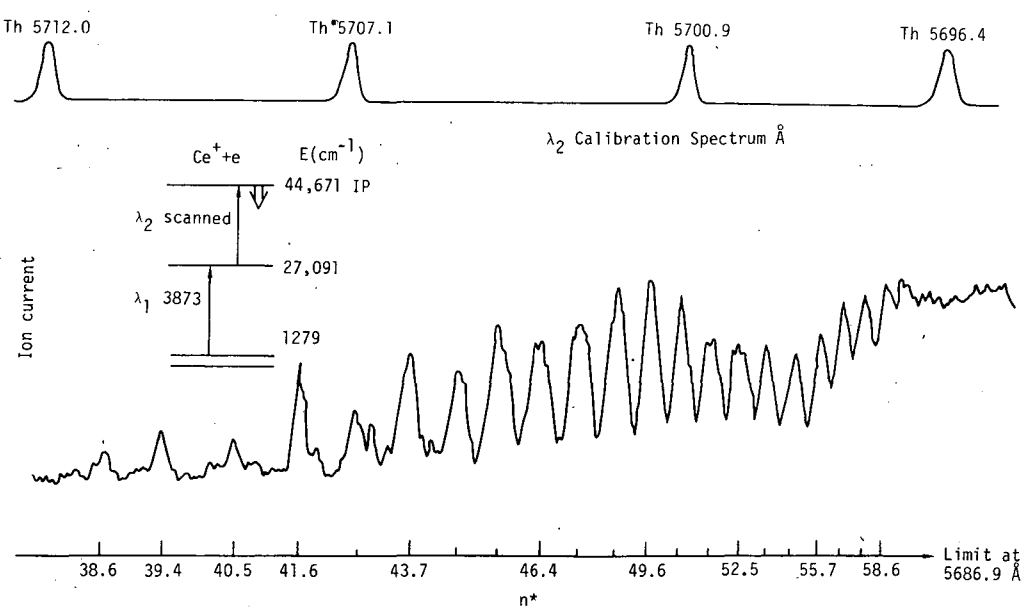

FIG. 8. Cerium series converging to the $^4H_{7/2}^o$ ground state obtained by pulsed field ionization (indicated by double arrow) of the bound Rydberg levels. The pulsed field of 100 V/cm was delayed 4 μs from the populating laser pulse.

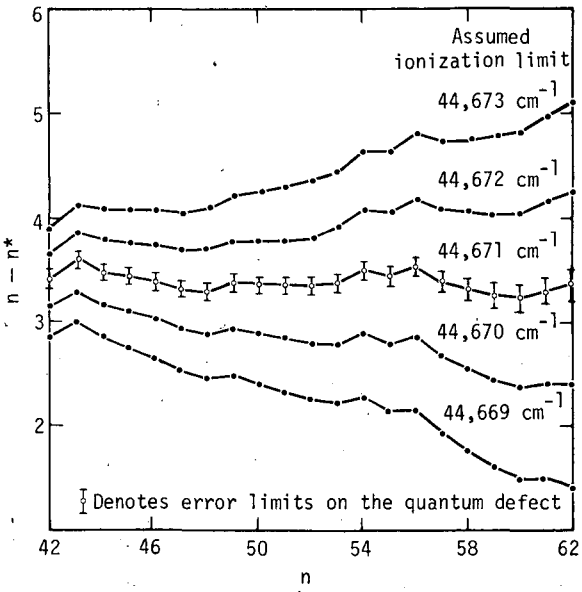

FIG. 9. Variation in quantum defect (n-n^*) vs n with change in assumed limit for the cerium Rydberg series shown in Fig. 8 (n and n^* are defined in the text). The assumed limit giving the most constant (n-n^*) value is (44 671 cm^{-1}) and it is taken as the ionization limit.

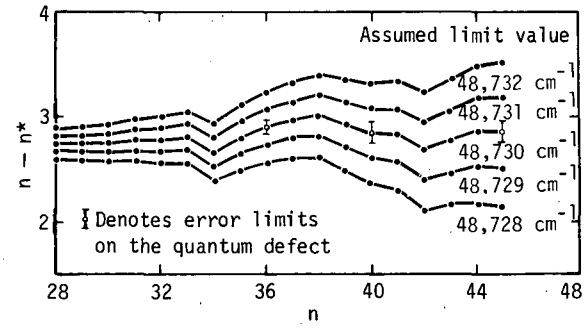

FIG. 10. Variation in quantum defect (n-n^*) vs n with change in assumed limit for one of the dysprosium double series shown in Fig. 6 (n and n^* are defined in the text). The assumed limit 48 730 cm^{-1} gives the most constant (n-n^*) value and when corrected by 828.31 cm^{-1} yields the ionization limit for dysprosium.

where R is the Rydberg constant. Our criterion for choosing the ionization limit of the element is to select the assumed limit that gives the smoothest and most constant value of the quantum defect as a function of n for the high quantum number Rydberg levels.[2,10] Figure 10 shows the same type plot for one of the double series in the dysprosium spectrum shown in Fig. 6.

We realize that our series are subject to perturbation by members of other Rydberg series and by certain valence levels. These can cause variations in the quantum defect from level to level. For the high principal quantum number levels involved here, such deviations are unlikely to cause errors larger than a few wave numbers between the chosen limit and the true limit. In cases where such perturbations are evident we have adopted larger uncertainties for the ionization limit.[16]

The Rydberg convergence limits derived from the observed series by this method are given in Table III. The excitation wavelengths and levels from which the series were observed and the ion levels that they converge to are indicated in the table. Information on ionic states was obtained from the literature for Nd,[17] Sm,[18] Eu,[19] Dy,[20] Ho,[21] and Er.[22] The fact that perturbations do not affect the measured limits by more than the quoted uncertainties is verified by the agreement of the limits determined from different parent levels (different series) of a given element. In some cases, the series are of different parity. In addition, the ionization limits obtained

TABLE III. Some lanthanide Rydberg series limits determined by stepwise laser spectroscopy techniques. The numbers in parentheses in the table indicate the uncertainty in the last digit of the value.

Element	λ_1^a (Å)	$\lambda_2^{a,b}$ (Å)	Excited level used (cm^{-1})	Convergence energy (cm^{-1})	Convergence level in ion[c] (cm^{-1})	First ionization limit[d] (cm^{-1})	(eV)
Ce	3793.83		26 331.11	44 674(3)	0.00	44 674(3)	5.5389(4)
	3873.03		27 091.56	44 671(3)	0.00	44 671(3)	5.5385(4)
Nd	4924.53		20 300.84	45 075(5)	513.32	44 562(5)	5.5250(6)
Sm	4596.74		22 041.02	45 846(5)	326.64	45 519(5)	5.6437(6)
Eu	4594.03		21 761.26	47 403(2)	1669.21	45 734(2)	5.6703(3)
	4661.88		21 444.58	47 405(2)	1669.21	45 736(2)	5.6706(3)
	6291.34	6787.48	30 619.49	47 403(2)	1669.21	45 734(2)	5.6703(3)
Gd	5617.91	6351.72	33 534.71	49 603(5)	0.00	49 603(5)	6.1501(6)
	5701.35	6573.83	32 957.77	49 604(5)	0.00	49 604(5)	6.1502(6)
Tb	4139.06		24 438.76	47 295(5)	0.00	47 295(5)	5.8639(6)
	4146.96		24 392.75	47 294(5)	0.00	47 294(5)	5.8638(6)
Dy	4211.72		23 736.60	48 730(5)	828.31	47 902(5)	5.9391(6)
	6259.09	6769.79	30 739.79	48 727(5)	828.31	47 899(5)	5.9388(6)
Ho	4103.38		24 360.55	49 203(8)	637.4	48 566(8)	6.0216(10)
	6305.36	6947.1[e]	30 246(2)	48 567(5)	0.00	48 567(5)	6.0216(6)
Er	4087.63		24 457.15	49 704(8)	440.43	49 264(8)	6.1080(10)
	6221.02	6451.56	31 565.94	49 699(8)	440.43	49 259(8)	6.1074(10)

[a]Excitation wavelengths (λ_1 and λ_2) and excited level values given to 0.01 are from Ref. 15 and references therein.
[b]No value of λ_2 is given for two step observations when λ_2 is scanned. Values given are λ_2 for three step results.
[c]Level values are from the following references: Nd, Ref. 17; Sm, Ref. 18; Eu, Ref. 19; Dy, Ref. 20; Ho, Ref. 21; and Er, Ref. 22.
[d]8065.479 cm^{-1}/eV used to convert values for cm^{-1} to eV.
[e]This excited level wavelength and energy were determined by laser techniques, Ref. 12.

TABLE IV. Summary of lanthanide first potentials.

Element	Electron[a] impact	Spectroscopic[b]	Laser spectroscopy LLL Photoionization threshold	Laser spectroscopy LLL Rydberg convergence	Rydberg convergence others
Ce	5.44(10)	5.466(20)	5.537(5)	5.5387(4)	
Pr	5.37(10)	5.422(20)	5.464($^{+12}_{-2}$)	[5.473(10)][c]	
Nd	5.49(10)	5.489(20)	5.523(2)	5.5250(6)	
Pm	...	5.554(20)	...	[5.582(10)][c]	
Sm	5.58(10)	5.631(20)	5.639(2)	5.6437(6)	
Eu	5.68(10)	5.666(7)	5.666(4)	5.6704(3)	5.670 45(3)[d]
Gd	6.24(10)	6.141(20)	...	6.1502(6)	
Tb	5.84(10)	5.852(20)	...	5.8639(6)	
Dy	5.90(10)	5.927(8)	5.936(3)	5.9390(6)	
Ho	5.99(10)	6.018(20)	6.017(3)	6.0216(6)	
Er	5.93(10)	6.101(20)	6.104(2)	6.1077(10)	
Tm	6.11(10)	6.18(2)	...	...	6.184 36(6)[e]
Yb	6.21(10)	6.25(2)	...	...	6.253 94(25)[e]

[a]Reference 14. This reference also contains a collection of limits determined by other techniques up until 1975.
[b]Reference 1. This reference is a collection of the best available limits derived by spectroscopic techniques up to the date of publication in 1974. The Tm and Yb Rydberg convergence values are given in the last column and are replaced here by values of Reader and Sugar from Ref. 13.
[c]Interpolated value from equation in Fig. 11 (see text).
[d]Reference 3.
[e]References 4 and 5.

in holmium from series converging to different limits agree well within the quoted uncertainty. The reliability of the method is also substantiated by the excellent agreement between our value of 45 734 ± 2 cm^{-1} for the ionization potential for europium and the more accurate value of 45 734.9 ± 0.2 cm^{-1} determined by Smith and Tomkins[3] using conventional high-resolution absorption spectroscopy.

DISCUSSION

A summary of lanthanide ionization limits obtained by various methods is given in Table IV. The latest electron impact values have the largest uncertainties of the values given in the table but they agree with the accurate Rydberg convergence limits within their quoted uncertainties except for erbium. Surface ionization results,[23] not shown here, have about the same uncertainties as the electron impact results and agree within the uncertainties with the Rydberg convergence values except for thulium and ytterbium where they are lower than the accurate values of Camus.[4,5] The spectroscopic values by Martin *et al.*[1] that include numerous semiempirical values by Reader and Sugar are in excellent agreement with our Rydberg convergence limits from samarium through erbium, but their cerium, praseodymium and neodymium values are low.

Photoionization threshold values are listed for eight lanthanides in Table IV. Values are not reported for gadolinium and terbium because these elements were measured last and we were able to interpolate values to estimate the wavelength ranges to search for Rydberg series in these elements. A comparison of our threshold and Rydberg convergence limits reveals that the threshold limits are lower by some 15–40 cm^{-1} (0.002 to 0.005 eV) in every case, see Tables I–IV. The Rydberg convergence limits for neodymium and europium are indicated by an arrow lableled R.L. on the photoionization threshold spectra shown in Figs. 3 and 4. As is the case in the neodymium scans shown, the Rydberg convergence limit generally occurs above the first apparent autoionization peak or peaks in all cases except europium. However, the first very strong autoionization peak always occurs at or above the Rydberg convergence limit, see Figs. 3 and 4. In our uranium investigation[10] a similar difference between the limits was found and remains an unexplained experimental discrepancy. Stray electric fields, the effect of intense laser radiation, and collisional effects are all possible explanations. In all cases we believe that the Rydberg convergence limit values are the most precise and they are the preferred values. For praseodymium no Rydberg series were found and only the photoionization threshold results are available. The uncertainties for the reported values are set as −0.002 to +0.012 eV (−20, +100 cm^{-1}) because the threshold values for all the lanthanides appear low with respect to the more accurate Rydberg convergence limits.

In the table, we also include an interpolated value for praseodymium as well as for promethium. We believe these are the most accurate estimates for the ionization potentials of these two elements. The interpolated values were obtained from an equation derived from a least-squares fit of the experimental ionization potentials discussed below.

With the exception of cerium and gadolinium, the ionization process in the lanthanides is the removal of an s electron from the $4f^N6s^2$ configuration with N equal to 2 through 14. That is, the ionization potential is the energy required to remove an s electron from an atom in the lowest level of the f^Ns^2 configuration and produce an ion in the lowest level of the f^Ns configuration. The ionization processes in cerium ($N = 2$) and gadolinium ($N = 8$) correspond to $f^{N-1}ds^2 \rightarrow f^{N-1}d^2$ and $f^{N-1}ds^2 \rightarrow f^{N-1}ds$, respectively.[15] However, these ionization limits can be corrected to correspond to the process $f^Ns^2 \rightarrow f^Ns$ by use of the very accurately known positions of the lowest levels of the f^Ns^2 and f^Ns configurations in the neutral and singly ionized atoms of cerium[24,25] and gadolinium.[26,27] Thus all these ionization potentials can be normalized to correspond to the removal of an s electron from the lowest level of the f^Ns^2 configuration. The resulting normalized ionization limits are plotted as a function of N in Fig. 11, and clearly show a con-

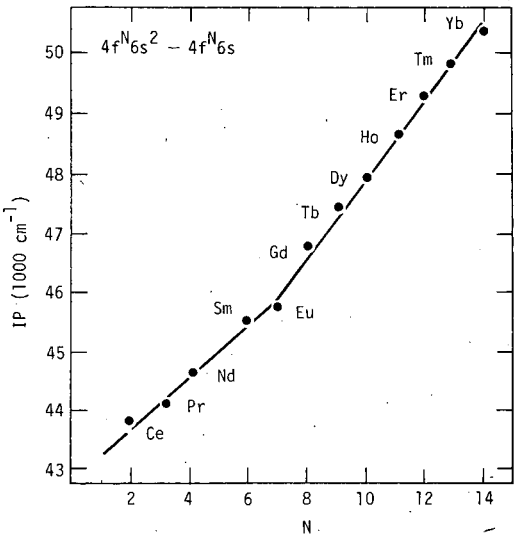

$$IP = \begin{cases} 441N + 42822\ \text{cm}^{-1} & \text{for } N \leq 7 \\ 661N + 41280\ \text{cm}^{-1} & \text{for } N \geq 7 \end{cases}$$

FIG. 11. Normalized ionization potentials of the lanthanides plotted as a function of number of f electrons. Only the Ce and Gd points required normalization to the $4f^N6s^2 \rightarrow 4f^N6s$ process, see text.

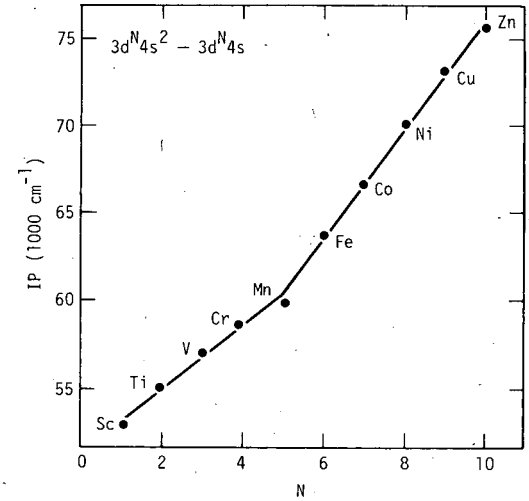

$$IP = \begin{cases} 1824N + 51333\ \text{cm}^{-1} & \text{for } N \leq 5 \\ 3117N + 44867\ \text{cm}^{-1} & \text{for } N \geq 5 \end{cases}$$

FIG. 12. Normalized ionization potentials of the $3d$ series. Corrections were necessary for V, Cr, Co, Ni, and Cu to normalize the ionization process to $3d^N4s^2 \rightarrow 3d^N4s$.

nected two-straight-line behavior with a change in slope at the half-filled shell ($N = 7$). The limits for thulium and ytterbium are Camus' values.[4,5] The solid line in the figure is an unweighted least-squares fit to the experimental data using a connected two-straight-line equation. The resulting numerical fit is shown at the bottom of this figure. The first half of the series fits to a slope of 441 cm^{-1} with a standard deviation of 19 cm^{-1} and the second half of the series to a slope of 661 cm^{-1} with a standard deviation of 14 cm^{-1}. The experimental normalized ionization values have a standard deviation of ±84 cm^{-1} from the solid line.

We have not included the lanthanum ($N = 1$) $f^Ns^2 \rightarrow f^Ns$ normalized ionization limit (43 932 ± 5 cm^{-1}) because the $^2F_{5/2}$ lowest level of the $4f6s^2$ configuration of the neutral atom at 15 196.80 cm^{-1} above the $5d6s^2$ ground state is severely mixed with neighboring levels of other odd configurations.[6,28] Because the position of this level is perturbed,[29] the normalized ionization limit is not expected to fall on the line defined by the other members of the series. In fact, it lies 669 cm^{-1} above the extrapolated value of 43 263 cm^{-1}.

The linear dependence on N with a slope break at the half-filled shell for the $l^Ns^2 \rightarrow l^Ns$ ionization process is not confined to the lanthanide series as we find the same behavior for the $3d$ and $4d$ series elements and for the $s^2l^N \rightarrow sl^N$ ionization process for the $2p$ and $3p$ series elements. The plot for the $3d$ or iron series is shown in Fig. 12. Again, the connected two-straight-line behavior with a slope change at the half-filled shell is shown.

A theoretical explanation of the behavior of the $l^Ns^2 \rightarrow l^Ns$ and also the $l^Ns \rightarrow l$ ionization potentials is given in a paper to appear shortly in this journal.[30] There it will be shown that the change in slope at the half-filled shell is equal to $G_l^{\text{ion}}(l,s)$. The difference in slope between the two lines in Fig. 11 is 220 ± 23 cm^{-1}. This is in good agreement with the average experimental value of $G_3(fs) = 205 \pm 6$ cm^{-1} for the lanthanides.[31]

Our treatment of the data in terms of the normalized ionization limits as a function of N is called horizontal analysis. Extensive horizontal analyses of energy differences between various configurations have been performed for the lanthanides[6,28,32,33] and actinides[32,33] as well as for the p and d series elements.[34–36] Systematic variations have been found that allowed predictions of energy levels and aided in the analyses of spectra. With the exception of Zollweg,[36] systematic trends in the $l^Ns^2 \rightarrow l^Ns$ ionization limits have not been studied. Zollweg considered the energy differences between the lowest levels of d^Ns^2 of the neutral and d^Ns of the ion but failed to recognize the connected two straight line behavior. Instead he assumed that the variation with N of the normalized ionization limit was quadratic.

CONCLUSIONS

Laser spectroscopy methods have been used to obtain ionization thresholds and to observe Rydberg series in a number of lanthanides with complex spectra. The ionization limits we determined for nine of the lanthanides have typical accuracies of 0.0006 eV and are 10–100 times more precise than values previously available. These values when combined with values previously determined for the other lanthanides[1–5] make accurate experimental ionization potentials available for all the lanthanides except promethium. These accurate limits led to the discovery of the connected two-straight-line behavior of the $l^Ns^2 \rightarrow l^Ns$ ionization potentials across the $4f$ series and then in other series (p and d) of the periodic table. This systematic variation of the ionization potential can be used to interpolate values and to aid in the analysis of spectra.

ACKNOWLEDGMENTS

We gratefully acknowledge technical support from S. A. Johnson, C. A. May, G. P. Vayer, and D. O. Kippenhan. Numerous discussions with K. Rajnak and B. W. Shore con-

cerning the theoretical interpretation and physical meaning of the regularities in the ionization potentials were very beneficial. We appreciate helpful contributions by L. R. Carlson and W. C. Martin, and thank J. Sugar for encouraging us to undertake the investigation of lanthanide ionization limits.

*Work performed under the auspices of the U.S. ERDA under contract No. W-7405-Eng-48.

[1]W. C. Martin, L. Hagan, J. Reader, and J. Sugar, "Ground levels and ionization potentials for lanthanide and actinide atoms and ions," J. Phys. Chem. Ref. Data **3**, 771–780 (1974).

[2]W. R. S. Garton and M. Wilson, "Autoionization-Broadened Rydberg Series in the Spectrum of LaI," Astrophys. J. **145**, 333–336 (1966).

[3]G. Smith and F. S. Tomkins, "Autoionization resonances in the EuI absorption spectrum and a new determination of the ionization potential," Proc. R. Soc. Lond., **342**, 149–156 (1975); G. Smith and F. S. Tomkins, "The absorption spectrum of europium," Philos. Trans. R. Soc. A **283**, 345–365 (1976).

[4]P. Camus, "Etude des spectres d absorption de l'ytterbium du lutecium et du thulium entre 2700 Å et 1900 Å," Thesis, Univ. Paris, Orsay (1971) 126–334 (unpublished).

[5]P. Camus and F. S. Tomkins "Spectre d'Absorption de Yb I," J. Phys. (Paris) **30**, 545–550 (1969).

[6]J. Blaise, P. Camus, and J. F. Wyart, "Seltenerdelemente, Sc Y, La and Lanthanide" in *Gmelin Handbuch der Anorganishen Chemie*, System No. 39 (Springer Berlin, 1976).

[7]A. C. Parr and F. A. Elder, "Photoionization of ytterbium: 1350–2000 Å," J. Chem. Phys. **49**, 2665–2667 (1968).

[8]A. C. Parr, "Photoionization of europium and thulium: Threshold to 1350 Å," J. Chem. Phys. **54**, 3161–3167 (1971).

[9]A. C. Parr and M. G. Inghram, "Photoionization of samarium in the threshold region," J. Opt. Soc. Am. **65**, 613–614 (1975).

[10]R. W. Solarz, C. A. May, L. R. Carlson, E. F. Worden, S. A. Johnson, J. A. Paisner, and L. J. Radziemski, "Detection of Rydberg states in uranium using time-resolved stepwise laser photoionization," Phys. Rev. A **14**, 846–853 (1976).

[11]F. B. Dunning and R. F. Stebbings, "Role of autoionization in the near-threshold photoionization of argon and krypton metastable atoms," Phys. Rev. A **9**, 2378–2382 (1974); R. D. Rundel, F. B. Dunning, H. C. Goldwire, and R. F. Stebbings, "Near-threshold photoionization of xenon metastable atoms," J. Opt. Soc. Am. **65**, 628–633 (1975).

[12]L. R. Carlson, J. A. Paisner, E. F. Worden, S. A. Johnson, C. A. May, and R. W. Solarz, "Radiative lifetimes, absorption cross sections, and the observation of new high-lying odd levels of ^{238}U using multistep laser photoionization," J. Opt. Soc. Am. **66**, 846–853 (1976).

[13]J. Reader and J. Sugar, "Ionization Energies of the Neutral Rare Earths," J. Opt. Soc. Am. **56**, 1189–1194 (1966).

[14]R. J. Ackermann, E. G. Rauh, and R. J. Thorn, "The Thermodynamics of ionization of gaseous oxides; the first ionization potentials of the lanthanides metals and monoxides," J. Chem. Phys. **65**, 1027–1031 (1976).

[15]W. F. Meggers, C. H. Corliss, and B. F. Scribner "Tables of Spectral-Line Intensities, Part I arranged by Wavelength," Natl. Bur. Stard. U.S. Monogr. **145** (1975).

[16]A much better procedure for handling perturbed series would be to analyze them using the methods of multichannel channel quantum defect theory (MQDT). See K. T. Lu and U. Fano, "Graphic Analysis of Perturbed Rydberg Series," Phys. Rev. **A2**, 81–86 (1970). The data we obtained in this investigation of the lanthanides are not amenable to such an analysis because no attempt was made to J select the observed states and the resolution used was insufficient to separate the many near-degenerate states that comprise the high principal quantum number Rydberg levels into the different total angular momentum states for identification with various couplings to the ionic core and the running electron. Recent high resolution (0.03 cm^{-1}) laser spectra of uranium have allowed application of MQDT. The results yielded a more accurate value for the ionization limit of uranium that agrees within the quoted uncertainty with our value for uranium (Ref. 10) obtained using techniques and lasers similar to those used to obtain our lanthanide results.

[17]W. E. Albertson, G. R. Harrison, and J. R. McNally, Jr., "First spark spectrum of neodymium-preliminary classification and Zeeman effect data" Phys. Rev. **61**, 167–174 (1942); P. Schruumans "On the Spectra of Neodymium and Uranium," Physica (Utr.) **11**, 419–425 (1946).

[18]W. E. Albertson, "Analysis of the spectrum of singly ionized samarium," Astophys. J. **84**, 2671 (1936).

[19]H. N. Russell, W. Albertson, and D. N. Davis "The spark spectrum of europium, Eu II," Phys. Rev. **60**, 641–656 (1941).

[20]J. G. Conway and E. F. Worden, "Preliminary level analysis of the first and second spectra of dysprosium, Dy I and II," J. Opt. Soc. Am. **61**, 704–726 (1971).

[21]J. Sugar, "Nuclear magnetic dipole moment of ^{165}Ho," J. Opt. Soc. Am. **58**, 1519–1523 (1968); A. E. Livingston and E. H. Pinningston, "Spectra of neutral and singly ionized holmium," J. Opt. Soc. Am. **61**, 1429–1430 (1971).

[22]J. R. McNally and K. L. Vander Sluis, "Preliminary classification of the spectrum of singly ionized erbium (Er II)," J. Opt. Soc. Am. **49**, 200L (1959).

[23]G. R. Hertel, "Surface ionization III. The first ionization potentials of the lanthanides," J. Chem. Phys. **48**, 2053–2058 (1968).

[24]W. C. Martin, "Low energy levels of neutral cerium," J. Opt. Soc. Am. **53**, 1047–1050 (1963) and "Low energy level structure of neutral cerium (Ce I)," Phys. Rev. A**3**, 1810–1815 (1971).

[25]C. H. Corliss, "Wavelengths and Energy Levels of the Second Spectrum of Cerium," J. Res. Nat. Bur. Stand. **77A**, 419–546 (1973).

[26]Th. A. M. Van Kleef, J. Blaise and J. F. Wyart, "Analysis of the Arc Spectrum of Gadolinium (Gd I)," J. Phys. (Paris) **32**, 609–615 (1971).

[27]J. Blaise and Th. A. M. Van Kleef, "Resultats nouvioux dans l'etude du spectre d'etincelle du gadolinium," C.R. Acad. Sci. B. **268**, 792–795 (1969).

[28]W. C. Martin, "Energy Differences between two spectroscopic systems in neutral, singly ionized and doubly ionized lanthanide atoms," J. Opt. Soc. Am. **61**, 1862–1866 (1971).

[29]Hannah Crosswhite in private communication (1977) indicated that the position of the lowest level of $4f6s^2$ could be affected by several hundred wave numbers by configuration interaction.

[30]K. Rajnak and B. W. Shore "Regularities in the s-electron binding energies in $l^N s^M$ configurations" J. Opt. Soc. Am. (to be published).

[31]B. G. Wybourne, *Spectroscopic Properties of the Rare Earths* (Wiley, New York, 1965), p. 56; see also Ref. 20, p. 725 and reference cited there.

[32]L. Brewer, "Energies of the Electronic Configurations of the Lanthanide and Actinide Neutral Atoms," J. Opt. Soc. Am. **61**, 1101–1111 (1971) and "Energies of the electronic configurations of the singly, doubly and triply ionized lanthanides and actinides," J. Opt. Soc. Am. **61**, 1666–1682 (1971).

[33]L. J. Nugent and K. L. Vander Sluis, "Theoretical treatment of the energy differences between $f^q d^1 s^2$ and $f^{q+1} s^2$ electron configurations for lanthanide and actinide atomic vapors," J. Opt. Soc. Am. **61**, 1112–1115 (1971).

[34]B. Edlen, "Handbuch der Physik," edited by S. Flugge (Springer, Berlin, 1964), Vol. 27, p. 80–220.

[35]M. A. Catalan, F. Rohrlich and A. G. Shenstone, "Relations between the low atomic configurations in the long periods," Proc. R. Soc. A **221**, 431–437 (1954).

[36]R. J. Zollweg, "Electron affinities of the heavy elements," J. Chem. Phys. **50**, 4251–4261 (1969).

This report was done with support from the Department of Energy. Any conclusions or opinions expressed in this report represent solely those of the author(s) and not necessarily those of The Regents of the University of California, the Lawrence Berkeley Laboratory or the Department of Energy.

TECHNICAL INFORMATION DEPARTMENT
LAWRENCE BERKELEY LABORATORY
UNIVERSITY OF CALIFORNIA
BERKELEY, CALIFORNIA 94720